Journal of Applied Polymer Science

Removal of Cd^{2+}, Cu^{2+}, Ni^{2+}, and Pb^{2+} Ions from Aqueous Solutions Using Tururi Fibers as an Adsorbent

Diego Q. Melo,[1] Carla B. Vidal,[2] André Leandro da Silva,[3] Raimundo N. P. Teixeira,[2] Giselle Santiago Cabral Raulino,[2] Thiago C. Medeiros,[1] Pierre B. A. Fechine,[1] Selma Elaine Mazzeto,[3] Denis De Keukeleire,[4] Ronaldo F. Nascimento[1]

[1]Department of Analytical Chemistry and Physical Chemistry, Federal University of Ceará, Fortaleza, Ceará, Brazil
[2]Department of Hydraulic and Environmental Engineering, Federal University of Ceará, Fortaleza, Ceará, Brazil
[3]Department of Organic and Inorganic Chemistry, Federal University of Ceará, Fortaleza, Ceará, Brazil
[4]Faculty of Pharmaceutical Sciences, Laboratory of Pharmacognosy and Phytochemistry, University of Gent, 9000 Gent, Belgium
Correspondence to: R. F. Nascimento (E-mail: ronaldo@ufc.br)

ABSTRACT: This work investigates the removal of Cd^{2+}, Cu^{2+}, Ni^{2+}, and Pb^{2+} ions from aqueous solutions using tururi fibers as an adsorbent under both batchwise and fixed-bed conditions. It was found that modification of the tururi fibers with sodium hydroxide increased the adsorption efficiencies of all metal ions studied. The fractional factorial design showed that pH, adsorbent mass, agitation rate, and initial metal concentration influenced each metal adsorption differently. The kinetics showed that multi-element adsorption equilibria were reached after 15 min following pseudo-second-order kinetics. The Langmuir, Freundlich, and Redlich–Peterson models were used to evaluate the adsorption capacities by tururi fibers. The Langmuir model was found to be suitable for all metal ions. Breakthrough curves revealed that saturation of the bed was reached in 160.0 mL with Cd^{2+} and Cu^{2+}, and 52.0 mL with Ni^{2+} and Pb^{2+}. The Thomas model was applied to the experimental data of breakthrough curves and represented the data well.
 J. Appl. Polym. Sci. **2014**, *131*, 40883.

KEYWORDS: adsorption; applications; cellulose and other wood products; separation techniques

Received 18 February 2014; accepted 13 April 2014
DOI: 10.1002/app.40883

INTRODUCTION

Metal ions may be present in toxic concentrations in the air due to the incineration of municipal and industrial wastes as well as in water intoxicated by industrial effluents. This context, the industry of metal finishing and electroplating units are one of the major sources of pollutants which contribute greatly to the pollution load of the receiving water bodies and therefore increase the environmental risks.[1–3] The metal concentrations vary greatly. However, on average concentrations range 20–600 mg L^{-1}.[4] Thus, in the absence of degradation pathways, metal ions may accumulate in the environment. There are various technologies for removing toxic metal ions from aqueous solutions including chemical precipitation, reverse osmosis, ion flotation, evaporation, ion exchange, and adsorption, the latter being the most promising technique.[2]

Various lignocellulose-derived materials have been studied as adsorbents including cellulosic substrates,[3] sugar cane bagasse,[4,5] cashew bagasse,[6] and coconut shell.[2,7–9] A major advantage of using natural fibers as adsorbents is the ready availability of renewable sources in nature, the low costs, the biodegradability as well as the excellent mechanical properties.

Natural fibers of vegetable origin are complex composite materials, consisting primarily of cellulosic microfibrils in an amorphous matrix of lignin and hemicellulose. Originally from the Amazon estuary, the palm of ubuçu (*Manicaria saccifera*) carries fruits protected by a fibrous sheath called "tururi." Despite the fact that these fibers have economic importance in a number of commercial sectors, there are no studies known on their physical and chemical properties for potential use in adsorption processes. This work focuses on removal of Cd^{2+}, Cu^{2+}, Ni^{2+}, and Pb^{2+} ions from aqueous solutions using tururi fibers as an adsorbent.

MATERIALS AND METHODS

Materials

Analytical-grade chemicals and ultrapure water (Millipore Direct Q3 Water Purification System) were used to prepare the solutions. Multi-element stock solutions of Cd^{2+}, Cu^{2+}, Ni^{2+}, and Pb^{2+} (500 mg L^{-1}) were prepared with $Cd(NO_3)_2.4H_2O$,

Table I. Coded Factors Used in the 2^{4-1} Fractional Factorial Design for Studying the Adsorption of Cu^{2+}, Pb^{2+}, Ni^{2+}, and Cd^{2+} by Tururi Fibers

Code	Factor (unit)	(−)	0	(+)
A	pH	4.5	5.0	5.5
B	Adsorbent mass (mg)	50	100	150
C	Agitation rate (rpm)	100	150	200
D	Initial metal concentration (mg L^{-1})	100	300	500

$Cu(NO_3)_2.3H_2O$, $Ni(NO_3)_2.6H_2O$, and $Pb(NO_3)_2$ (Merck, São Paulo, Brazil), respectively. The acetate buffer was prepared with sodium acetate and glacial acetic acid. NaOH (0.10 mol L^{-1}) and HCl (0.10 mol L^{-1}) solutions were used for pH adjustments. Tururi fibers were supplied by Embrapa Tropical Agroindustry, CE, Brazil (EMBRAPA/CE).

Alkaline Treatments

Tururi fibers were treated with different concentrations of NaOH (5, 7, and 10% [w/v]) for 4 h at 60°C, then washed with deionized water until neutral, and dried at 60°C.

Adsorbent Characterization

Tururi fibers, before and after alkaline treatments, were analyzed by Fourier-transform infrared spectrophotometry in the ATR mode and in the wavenumber range from 500 cm^{-1} to 4000 cm^{-1} (Bruker model Vertex 70).

Experimental Design and Statistical Analysis

A fractional factorial design was conducted to study the influence of four factors in the multicomponent ion adsorption of Cu^{2+}, Pb^{2+}, Ni^{2+}, and Cd^{2+} using tururi fibers as adsorbent (Table I). Tururi fibers were added to multicomponent solutions (25.0 mL) in 50 mL Erlenmeyer flasks. The mixtures were mechanically stirred for 2 h at 28 ± 2°C.

The experiments were performed with two replications in the corner points (combinations of "−" and "+" levels) and four the central points. The adsorption capacity, q, of each metal and total adsorption capacity, q_{tot}, were the responses measured. The values of q were calculated using eq. (1). The total adsorption capacity, q_{tot}, was calculated using the following relationship:

$$q_{tot} = \sum_{j=1}^{4} \frac{(C_{0,j} - C_{e,j})}{W} V,$$

where $C_{0,j}$ is the initial metal ion concentration (given in units of mg L^{-1}), $C_{e,j}$ the equilibrium metal ion concentration (also given in mg L^{-1}), W the adsorbent mass (given in units of g), and V the volume (given in unit of L).

MINITAB statistical software (version 16) was used to design and analyze the fractional factorial experiments. The results were analyzed to estimate of the effects on the adsorption process. Data were reported as mean ± standard deviation at a significance level of $P < 0.05$. Pareto charts were constructed using the results of the Student's t-test. The results obtained were fit to mathematical models using analysis of variance.

Then, the experiments were performed in duplicate. The equilibrium adsorption capacities of the adsorbent were calculated using eq. (1):

$$q_e = \frac{(C_o - C_e)}{W} V \quad (1)$$

where q_e is the equilibrium adsorption capacity (milligram of metal per gram adsorbent), C_o is the initial concentration of the metal ion (mg L^{-1}), C_e is the equilibrium concentration of metal ion (mg L^{-1}), V is the volume of the solution (L), and W is the mass of adsorbent (g). Control experiments were performed in the absence of adsorbent to check for any adsorption on the walls of the flasks.

Adsorption Kinetics

Adsorption kinetics allow to evaluate the extent of removal of metal ions as well as to identify the prevailing mechanism(s) involved in the adsorption process. The multi-element solution was continuously shaken at pH 5.5 appropriate. Aliquots of the supernatant were collected at regular time intervals, up to 60 min. Adsorption capacities were calculated by the differences between the initial and the final concentrations at any given time.

The experimental data that were obtained from the adsorption kinetics were fit to pseudo-first-order [eq. (2)] and pseudo-second-order [eq. (3)] models[10]:

$$\log(q_e - q_t) = \log q_e - \left(\frac{K_1}{2303}\right) t \quad (2)$$

where q_e and q_t are the amounts of adsorbate that were retained (mg g^{-1}) at equilibrium and at any given time t (min), respectively, and K_1 is the rate constant for the pseudo-first-order model (min^{-1}).

$$\frac{t}{q_t} = \frac{1}{K_2 . q_e^2} + \frac{1}{q_e} t \quad (3)$$

where q_e and q_t are defined in eq. (3), and K_2 is the rate constant for the pseudo second-order model (g mg^{-1} min^{-1}).

Adsorption Isotherms

Tururi fibers were added to mono-element and multi-elements solutions in 50-mL Erlenmeyer flasks, with metal ion concentrations in the range of 20–500 mg L^{-1}, at pH appropriate. The data obtained for the adsorption isotherms were described according to the Langmuir [eq. (4)] and Freundlich [eq. (5)] models[11]:

$$q_e = \frac{q_{máx} K_L C_e}{(1 + K_L C_e)} \quad (4)$$

where C_e is the solute concentration at equilibrium (mg L^{-1}), q_e is the amount of metal ion that is adsorbed at equilibrium (mg g^{-1}), q_{max} is the monolayer capacity of the adsorbent

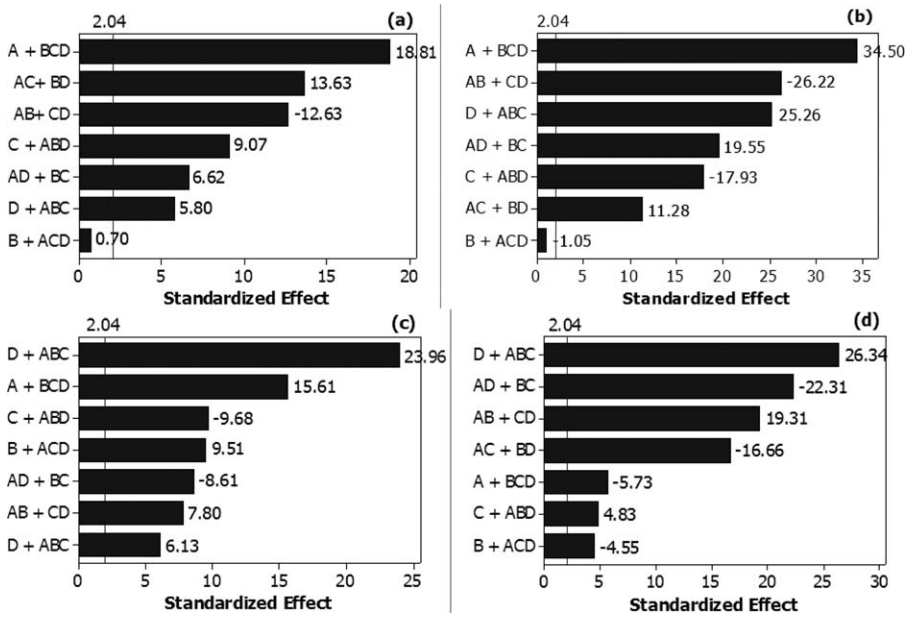

Figure 1. Standardized Pareto charts showing main effects of experimental parameters on responses at the confidence limit of 95% for: (a) $q_{Cu(II)}$, (b) $q_{Pb(II)}$, (c) $q_{Ni(II)}$, and (d) $q_{Cd(II)}$.

(mg g^{-1}), and K_L is the Langmuir adsorption constant, which is related to the energy of adsorption (L mg^{-1}).

$$q_e = K_f . C_e^{\frac{1}{n}} \tag{5}$$

where C_e and q_e are defined in [eq. (5)], and K_f (L mg^{-1}) and n are Freundlich adsorption isotherm constants related to the saturation capacity and intensity of adsorption, respectively.

For the adsorption study involving multi-element system was applied to extended Langmuir equation.

$$q = \frac{q_{\max} K_{L,i} C_i}{1 + \sum_{j=1}^{n} K_{L,j} C_j}, \tag{6}$$

where $j = 1, 2, \ldots, n$, with i and j representing the components of the solution; q is the adsorption capacity; $q_{\max}$ is the maximum adsorption capacity in a monoelement system, and K_L is the Langmuir constant.

Fixed-Bed Experiments

An adsorption column (9.5 cm height and 1.0 cm diameter) was prepared with the adsorbent (2 g). About 160 mL of the multi-element solution (300 mg L^{-1}) was passed through the column at a flow rate of 2.0 mL min^{-1} and samples of 4 mL each were collected at the outlet of the column prior to analyses. The results were used to build the breakthrough curves and to determine the breaking point.

Breakthrough curves were determined as the relationship between the concentration in the sample that had passed through the adsorbent and the initial concentration. For each sorbent/sorbate system, the retention parameters were determined from the appropriate curve.[8,12]

For an ideal breakthrough curve, C_o is the initial adsorbate concentration and V_e is the effluent volume that percolates through the column. The breakthrough point, chosen arbitrarily as C_b, occurs when the effluent concentration reaches 5% of the initial concentration C_o. The column achieves complete saturation when the concentration C_x approaches C_o. The total effluent volume, V_b, is passed through the column until the breakthrough point is reached.[13] The part between C_x (exhaustion point) and C_b (breakthrough point) is called the primary adsorption zone (PAZ) and the time needed to establish PAZ in the column is calculated by eq. (7)[8,14,15]:

$$t_x = \frac{V_x}{F_m} \tag{7}$$

where t_x is the time to establish PAZ (min), F_m is the flow rate (mL min^{-1}), and V_x is the exhaustion volume (mL).

The time required for movement of PAZ down the column is given by eq. (8)[14,15]:

$$t_\sigma = \frac{(V_x - V_b)}{F_m} \tag{8}$$

where t_σ is the time required for movement of PAZ down the column (min), V_b is the breakthrough volume (mL), F_m is the flow rate (mL min^{-1}), and V_x is the exhaustion volume (mL). Thus, for a depth D of the adsorbent, the depth and time ratios are given by eq. (9)[14,15]:

$$U = \frac{\delta}{D} = \frac{t\delta}{(t_x - t_f)} \tag{9}$$

where δ is the length of PAZ (cm), D is the adsorbent depth (cm), and t_f is the PAZ formation time. The time required to achieve PAZ is given by eq. (10)[14,15]:

$$t_f = (1 - F) t_\delta \tag{10}$$

where F is the column fractional capacity in the adsorption zone characterized by the solute adsorbed from the solution under limiting conditions.

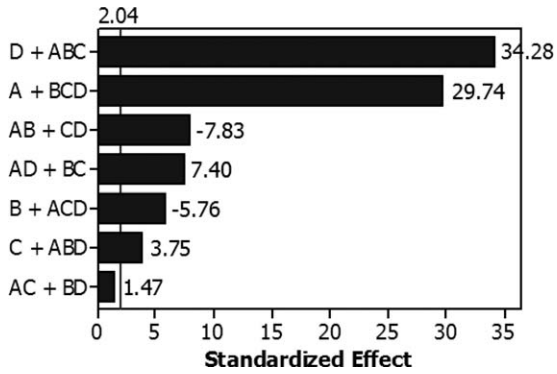

Figure 2. Standardized Pareto charts sowing main effects of experimental parameters on responses at the confidence limit of 95% for q_{tot}.

The column fractional capacity is given by eq. (11)[14,15]:

$$F = \int_{V_b}^{V} \frac{(C_o - C).d_v}{C_o(V_x - V_b)} \tag{11}$$

The column saturation percentage is obtained by eq. (12)[14,15]:

$$\%S = \left[1 - \frac{(\delta(F-1))}{D}\right] \times 100 \tag{12}$$

The maximum capacity of adsorption of metal ions on the column is given by eq. (13)[8,12]:

$$Q = \frac{C_o x F_m}{m_S} \int_{t=0}^{t=x} \left(1 - \frac{C}{C_o}\right) dt \tag{13}$$

where Q is the maximum adsorption capacity (mg g^{-1}); C_o is the initial concentration, C is the concentration of the adsorbate at a certain volume, m_s is the mass of adsorbent (g), F_m is the volumetric flow (L min^{-1}), and t is the time (min).

Although several models can be used to calculate kinetic constants and maximum adsorption capacities of a fixed-bed process, the Thomas model is mostly applied. The Thomas equation for an adsorption column can be expressed by eq. (14).

$$\frac{C_e}{C_o} = \frac{1}{1 + \exp\left(\left(\frac{K_{TH} q_{TH} m}{F}\right) - \frac{K_{TH} C_o V}{F}\right)} \tag{14}$$

where C_e is the effluent concentration (mg L^{-1}), C_o is the initial concentration (mg L^{-1}), F is the flow rate (mL min^{-1}), m is the mass of adsorbent (g), V is the volume (mL), and K_{TH} (L mg^{-1} min^{-1}), and q_{TH} (mg g^{-1}) are the adsorption kinetic rate constant and the maximum adsorption capacity of the column, respectively.

Non-Linear Regression

Linear regression is the most widely used method for the determination of isotherms parameters. The quality of a model is given by the values of the resulting determination coefficients, with a higher quality of the model being associated to determination coefficients closer to the unit.[16] However, some studies have warned about errors resulting from linearization methods, while considering that a non-linear approach should be robust and provide higher determination coefficients. Therefore, in this work, non-linear methods were used to determine the parameters of the Langmuir, Freundlich, and Redlich−Peterson isotherm models. The optimization procedure was performed for each experimental dataset using the solver add-in for Microsoft Excel and considering the values obtained for the sum of the squares of the errors (ERRSQ), the most widely used error function, represented by eq. (15).

$$ERRSQ = \sum_{i=1}^{p} (q_{exp} - q_{calc})_i^2 \tag{15}$$

where q_{exp} is the experimental value for each sample from the batchwise experiment and q_{cal} is the corresponding value, estimated with the isotherm model. All data presented are the mean values of two results obtained from identical essays. Variation coefficients were found to be lower than 5% and the statistical analyses were performed with Microsoft Excel software.

Metal Ions Quantitation

The concentrations of Cu^{2+}, Cd^{2+}, Ni^{2+}, and Pb^{2+} were measured with an atomic absorption spectrophotometer (933 plus, GBC, Sydney, Australia) using hollow cathode lamps and detection at wavelengths of 324.7 nm, 228.8 nm, 352.4 nm, and

Table II. Column Assignment for the Various Factors in the Fractional Factorial Design (2^{4-1}) and Experimental Values for Multicomponent Metal Ions Adsorption

	Coded factors								
Run	A	B	C	D[a]	$q_{Cu(II)}$	$q_{Pb(II)}$	$q_{Ni(II)}$	$q_{Cd(II)}$	q_{tot}
1	−	−	−	−	5.88 ± 1.45	14.56 ± 1.61	4.36 ± 0.77	2.60 ± 0.42	27.41 ± 1.57
2	+	−	−	+	16.95 ± 1.69	41.28 ± 0.95	22.19 ± 0.41	8.15 ± 0.51	88.57 ± 1.21
3	−	+	−	+	11.75 ± 1.73	25.61 ± 1.16	4.95 ± 1.20	10.26 ± 0.92	52.56 ± 3.54
4	+	+	−	−	5.54 ± 1.09	15.50 ± 0.40	8.04 ± 0.92	11.46 ± 0.21	40.53 ± 1.22
5	−	−	+	+	3.36 ± 0.74	6.16 ± 0.57	18.98 ± 1.04	24.25 ± 0.92	52.74 ± 2.89
6	+	−	+	−	21.77 ± 1.36	22.88 ± 1.57	8.98 ± 1.31	3.25 ± 1.15	56.88 ± 3.15
7	−	+	+	−	9.99 ± 0.48	13.12 ± 0.21	6.20 ± 0.58	1.87 ± 0.76	31.18 ± 1.33
8	+	+	+	+	22.00 ± 1.36	29.15 ± 0.53	21.10 ± 1.54	9.05 ± 0.43	81.29 ± 1.14
9	0	0	0	0	24.74 ± 1.39	26.60 ± 1.03	5.05 ± 1.55	4.79 ± 1.24	61.17 ± 3.15

[a] Generator: I = ABCD.

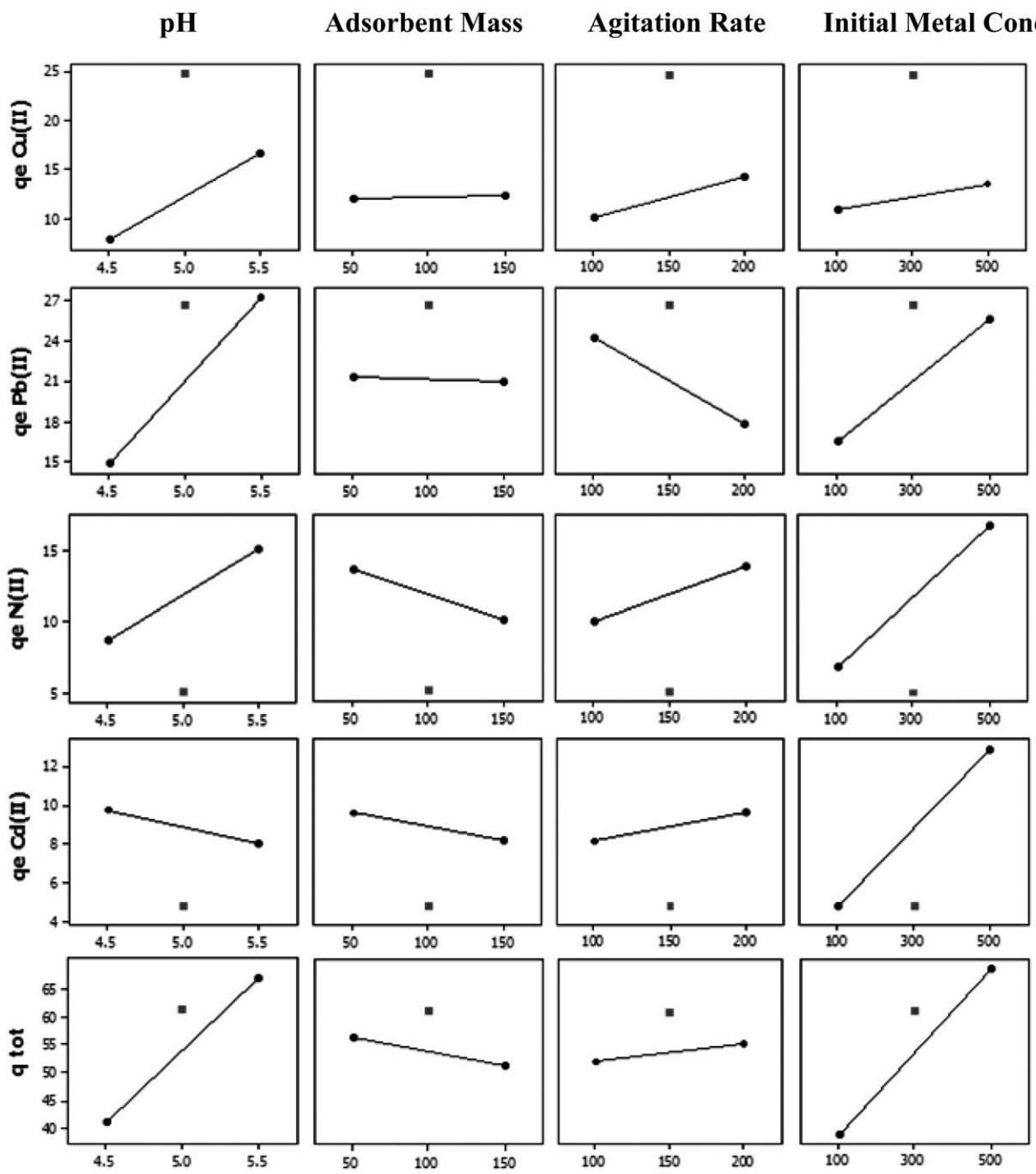

Figure 3. Factorial plots: main effects versus responses analyzed.

283.3 nm, respectively. Prior to analysis, samples were filtered and properly diluted with ultrapure water. The concentration of the analytes should fit the linear range of the calibration curves, which ranged from 1.0 to 5.0 mg L^{-1}, 0.2 to 1.8 mg L^{-1}, 6 to 28 mg L^{-1}, and 7 to 40 mg L^{-1} for Cu^{2+}, Cd^{2+}, Ni^{2+}, and Pb^{2+}, respectively.

RESULTS AND DISCUSSION

Influence of Alkaline Treatments

The tururi fibers were treated with sodium hydroxide at concentration levels from 0 to 10% (w/v) and the results are presented in Figure 1. The most effective removal of metal ions occurred at a concentration of 7%, with adsorption capacities (mg g^{-1}) around 14.4 for Cd^{2+}, 23.6 for Cu^{2+}, 14.7 for Ni^{2+}, and 28.0 for Pb^{2+}. The fibers modified with 7% (w/v) sodium hydroxide were used for subsequent experiments.

The results, shown in Figure 1, reveal that the adsorption capacities of the modified tururi fibers are much higher than those of the unmodified tururi fibers, which is likely due to the formation of additional hydroxyl groups in the cellulose-type core upon alkaline treatment. Also, the fine structure and the morphology of the fibers as well as the conformation of the

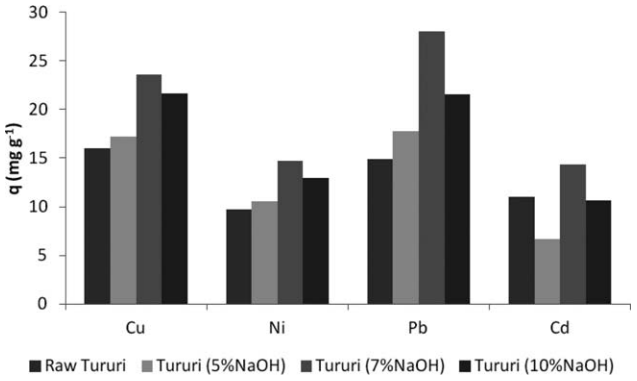

Figure 4. Adsorption capacities (mg g^{-1}) of metal ions versus concentration levels. Conditions: adsorbent dose (2.5 g L^{-1}), initial concentration (100 mg L^{-1}), contact time (4 h), pH (5.5), temperature (28 ± 2°C).

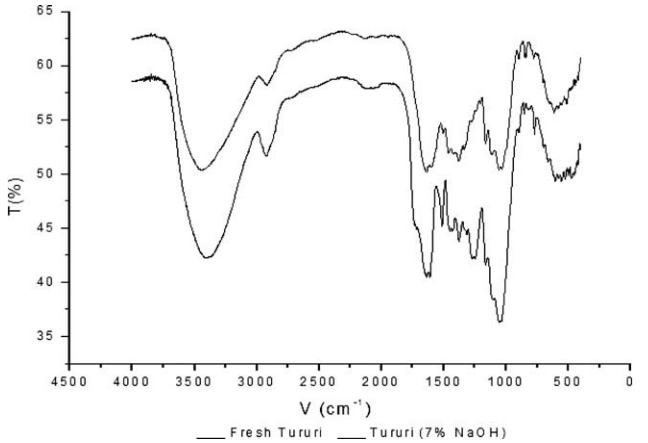

Figure 5. FTIR spectra of raw tururi fiber and modified tururi fiber (7% NaOH).

cellulose chains may be altered thereby facilitating their solubilization as well as removing components such as lignin and hemicelluloses.[2,17]

It is possible that the conversion of cellulose type I to type II has a considerable efficient in the presence of NaOH solution. Cellulose is transformed to sodium cellulose by treatment with concentrated NaOH solution, and then reverts to cellulose by washing. During this process, smaller hydrates of the sodium hydroxide dipole penetrate into the cellulose crystalline regions and destroy the strong intermolecular. Thus, the increase in adsorption capacity on tururi fibers submitted to alkaline treatment can be attributed to the formation of cellulose type II, which has more hydroxyl group available to react with the metal.[18]

Characterization of Tururi Fibers

FTIR spectra of the raw tururi fibers and the treated tururi fibers (7% NaOH), shown in Figure 2, indicate the presence of the same types of functional groups in both adsorbents. Following bands can be assigned: 3400 cm^{-1} (strong): stretching of hydroxyl groups, 2934 cm^{-1}: C—H stretching, 1607, 1511, 1427, and 1323 cm^{-1} (weak): aromatic skeletal vibrations, 1377 and 1247 cm^{-1}: C—H and C—O stretchings in the acetyl groups of hemicellulose, 1049 cm^{-1}: C—O and C—O—C stretchings in cellulose and hemicelluloses. The NaOH activation removes components such lignin and hemicelluloses. It can be observed in Figure 2 the picks high of C—O and C—O—C groups, related to lignin and hemicelluloses, suffered a decrease (1049 cm^{-1}) from raw tururi fibers.[8,17] From the functional groups present on the surface of the fibers may be suggested adsorption mechanism involved. The existence of hydroxyl and carboxyl groups suggests a mechanism for the chelation of metals such groups.

Results of the Experimental Design

The results obtained through the experimental design for multicomponent metal ions adsorption using tururi fibers are presented (Table II). It can be observed that the adsorption uptake of each metal is different depending on the conditions applied in the process. Some set of experimental conditions may favor the adsorption of a particular metal over others. Note that the combination of observations used in estimating the main effect of factor D (initial metal concentration) is identical to that used estimating the three-factor interaction effect of factors *A* (pH), *B* (adsorbent mass), and *C* (agitation rate); hence, estimates of factor *D* and the interaction effect of factors *A*, *B*, and *C* are said to be "confounded."[19] The used generator (*I* = *ABCD*) implies in alias structure in which the main effects are aliased with three-factor interaction effects, and two-factor interaction effects are confounded with each other. The higher order interaction effects (three- and four-factor interactions in this study) are often negligible and can be ignored.[20] Thus, the main effects can be obtained without confusion with higher order interaction effects. The two-factor interaction effects, though, are confounded and cannot be precisely estimated.

The Pareto charts of the experimental design are given in Figures 3 and 4. Observing Figure 3, it can be seen that the main effects influencing the responses $q_{Cu(II)}$ and $q_{Pb(II)}$ are *A* (pH), *C* (agitation rate), and *D* (initial metal concentration), while all main effects influence the responses $q_{Ni(II)}$ and $q_{Cd(II)}$. In fact,

Table III. Regression Equations of the Fitted Models in Terms of Coded Values

$q_{Cu(II)} = 24.74 + 4.41*A + 2.12*C + 1.36*D - 2.96*A*B + 3.19*A*C + 1.55*A*D - 12.58*CtPt$
$q_{Pb(II)} = 26.60 + 6.17*A - 3.21*C + 4.52*D - 4.69*A*B + 2.02*A*C + 3.50*A*D - 5.57*CtPt$
$q_{Pb(II)} = 26.60 + 6.17*A - 3.21*C + 4.52*D - 4.69*A*B + 2.02*A*C + 3.50*A*D - 5.57*CtPt$
$q_{Ni(II)} = 5.05 + 3.23*A - 1.78*B + 1.97*C + 4.95*D + 1.27*A*B - 2.00*A*C + 1.61*A*D + 6.80*CtPt$
$q_{Cd(II)} = 4.79 - 0.88*A - 0.70*B + 0.74*C + 4.06*D + 2.98*A*B - 2.57*A*C - 3.44*A*D + 4.07*CtPt$
$q_{tot} = 61.17 + 12.92*A - 2.50*B + 1.63*C + 14.89*D - 3.40*A*B + 3.22*A*D - 7.27*CtPt$

A = pH; *B* = adsorbent mass; *C* = agitation rate; *D* = initial metal concentration; CtPt = central point.

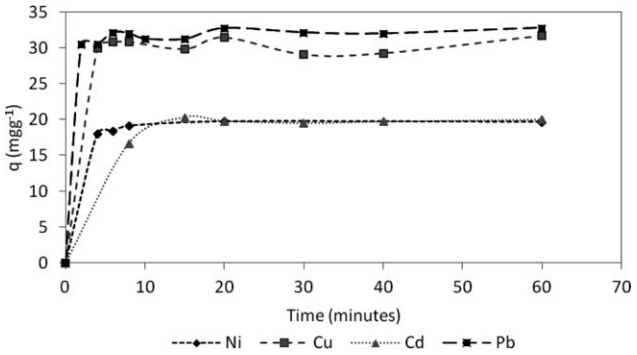

Figure 6. Multi-element adsorption kinetics for tururi fiber (7% NaOH) as an adsorbent.

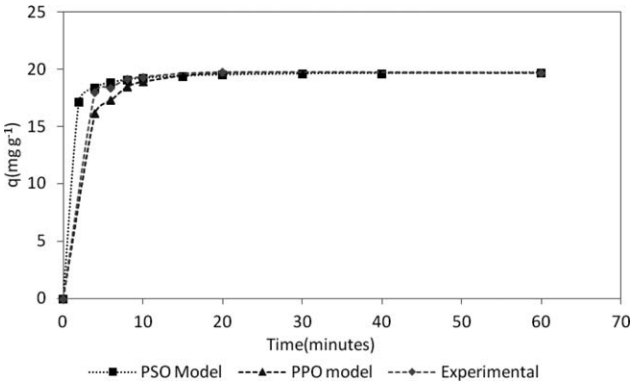

Figure 7. Kinetic models for adsorption of Ni^{2+} using tururi fiber as an adsorbent.

factor *B* (adsorbent mass) is supposed to influence in the adsorption uptake of all metal ions in mono-element solution. But in multi-element solution all metal ions are competing for the same adsorption sites. It means that in the multi-element system the increase in adsorbent mass seems not to influence in the adsorption uptake of Cu^{2+} and Pb^{2+} because the additional adsorption sites are being selectively occupied by Ni^{2+} and Cd^{2+}. As can be seen in Figure 4 all main effects influence in the total adsorption uptake, with the main effects *D* and *C* being the most influencing effects.

The main effect plots are used to understand how the variation in the levels of a factor affects the response. An examination of Figure 5 reveals how each variable affects the responses. The pH affects positively the responses $q_{Cu(II)}$, $q_{Pb(II)}$, $q_{Ni(II)}$, and q_{tot}, and affects negatively the response $q_{Cd(II)}$. Adsorbent mass affects negatively the responses $q_{Ni(II)}$, $q_{Cd(II)}$, and q_{tot}. Agitation rate affects positively the responses $q_{Cu(II)}$, $q_{Ni(II)}$, $q_{Cd(II)}$, and q_{tot}, and affects negatively the response $q_{Pb(II)}$. Initial metal concentration affects positively all responses analyzed.

Table III shows the regression equations for the five responses analyzed in the experimental design. The term CtPt in the equations is the curvature in the model introduced by the addition of a central point in the model. It indicates that the relationship between the variables is not linear. The fitted equations can be used to estimate the results of an adsorption experiment. The maximum of the model for total adsorption, q_{tot}, according to the fitted model, is obtained maintaining factors *A* (pH), *C* (agitation rate), and *D* (initial metal concentration) at higher level (+1) and factor *B* (adsorbent mass) at lower level (−1).

Adsorption Kinetics

The adsorption of metal ions by tururi fiber involves the coordination of these metal ions by oxygen, whose free electrons

Table IV. Parameters of the Models for Adsorption Kinetics

			Pseudo-first-order			Pseudo-second-order		
Metal ion	C_o	q_e	q_{cal}	K_1	R^2	q_{cal}	K_2	R^2
Ni^{2+}	100	19.69	19.69	0.59	0.9644	19.80	0.16	1.0000
Cu^{2+}	100	31.76	31.76	0.26	0.9532	31.65	0.06	0.9944
Cd^{2+}	100	20.00	19.38	0.07	0.8897	20.16	0.09	0.9982
Pb^{2+}	100	32.80	32.46	0.07	0.8739	32.70	0.10	0.9997

Table V. Parameters of the Models for Adsorption Isotherms

		Ni^{2+}	Cu^{2+}	Cd^{2+}	Pb^{2+}
Langmuir	q_{max}	50.12	36.36	156.87	346.28
	K_L	2.43×10^{-3}	1.7×10^{-2}	5.4×10^{-3}	6.93×10^{-3}
	R^2	0.98	0.99	0.97	0.99
	ERRSQ	8.02	8.65	273.00	446.98
Freundlich	K_F	0.978	6.84	2.95	5.33
	1/*n*	0.55	0.27	0.62	0.71
	R^2	0.96	0.96	0.93	0.97
	ERRSQ	15.53	25.63	733.40	630.54

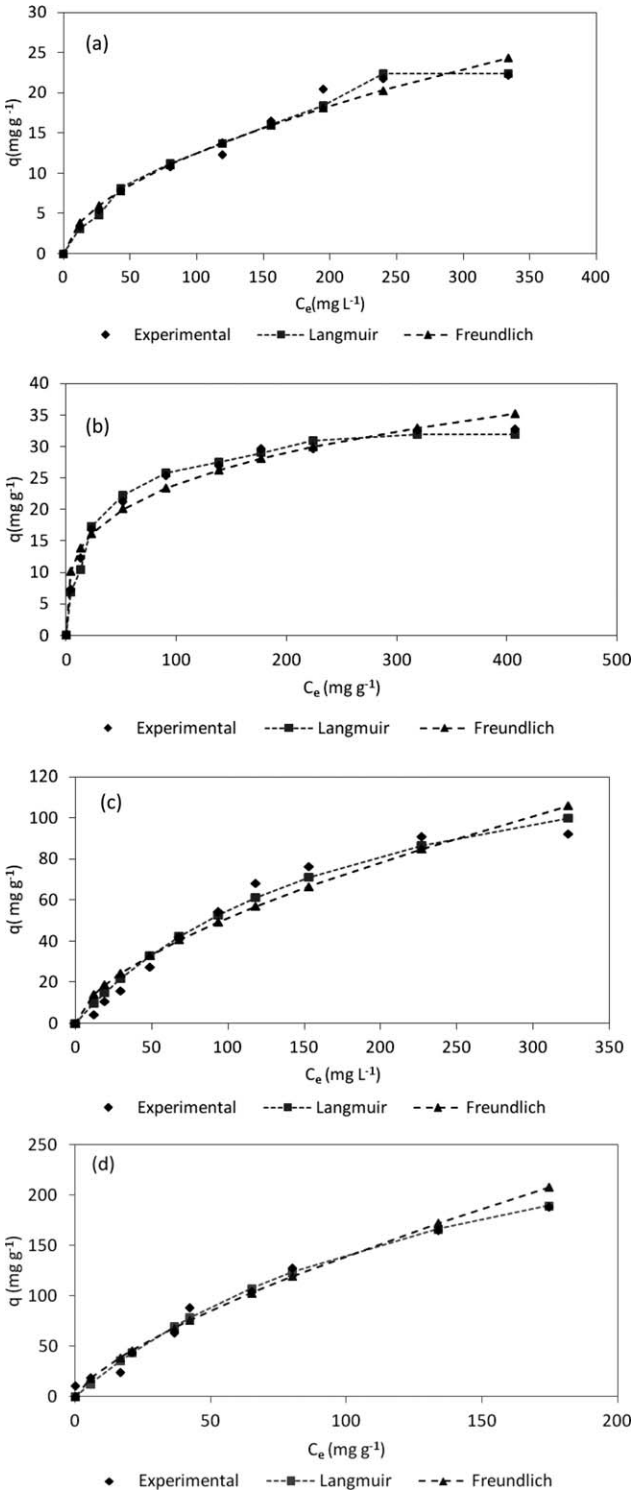

Figure 8. Isotherms for the adsorption of (a) Ni^{2+}, (b) Cu^{2+}, (c) Cd^{2+}, and (d) Pb^{2+}, by tururi fiber.

favor the formation of metal–adsorbent complexes onto the adsorbent surface. The adsorption kinetics are expressed as the solute removal rates that control the residence time of the adsorbate in the solid–solution interface. In practice, kinetics are studied in batchwise systems using various initial adsorbate concentrations, sorbent doses, temperatures, and adsorbate

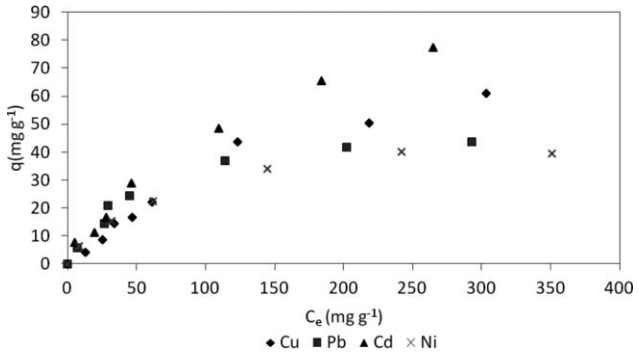

Figure 9. Experimental adsorption isotherms of Ni^{2+}, Cu^{2+}, Cd^{2+}, and Pb^{2+} from multi-element systems by fiber-treated tururi.

types to determine the times required to reach equilibrium.[12,20] The equilibrium times for the adsorption of metal ions onto tururi fibers (7% NaOH) were: 5 min for Cu^{2+}, Ni^{2+}, and Pb^{2+}, and 15 min for Cd^{2+} (Figure 6).

The adsorption kinetics are initially fast because adsorption takes place predominantly onto the outer surface, followed by a slow adsorption step onto the inner surface of the adsorbent.[13] A short time required to reach equilibrium, besides being beneficial to the process, is regarded as an indicator that the adsorption is controlled by chemical interactions rather than by diffusion.[21,22] Similar results have been reported by Teixeira et al.,[22] using alkaline-treated barley for the adsorption of Cu^{2+} from aqueous solutions.

Pseudo-first order (PFO), pseudo second-order (PSO), and models were applied to monitor the kinetics of the adsorption process(es) and the prevailing mechanism(s). Both angular and linear coefficients of the equations were used in the calculations of the constants K_1 and K_2, given in Table IV. The experimental values for the adsorption capacities values (q_e) were found to be in agreement with those of the theoretical adsorption capacities (q_c) that were calculated by the PSO model as supported by the R^2 values and error functions (Figure 7). Our results are in accordance with the adsorption of metal ions onto lignocellulosic materials following a pseudo-second-order model.[2,23–25] Results were also adjusted the diffusion models of Weber Morris[22] (not shown). However, the experimental data did not fit the model, indicating that the interaction between adsorbent and adsorbate occurs on the outer surface of the material.

Adsorption Isotherms

Adsorption isotherms of the metal ions studied onto tururi fibers (7% NaOH) were obtained by plotting the concentration of each metal ion adsorbed on the solid phase (q) versus its concentration in the liquid phase (C_e). The Langmuir and Freundlich models were applied to the experimental data in mono-element isotherms and the parameters determined for each model are given in Table V.

Evaluation of the experimental data by the theoretical models revealed that the Langmuir model adequately described the adsorption mechanism in a mono-element system for all metal ions studied (Figure 8), as shown by the values of the coefficients of determination R^2 and the error functions.

Table VI. Comparison of the Adsorption Capacities of Various Adsorbents

	Operational conditions		q_m (mg g^{-1})				
Adsorbent	pH	T (°C)	Ni^{2+}	Cu^{2+}	Cd^{2+}	Pb^{2+}	Reference
Tururi fiber	5.5	28	50.12	36.36	156.87	346.28	This study
Ulva lactuca	5.5	ambient		53.98	46.08	54.30	23
Rice straw	6	60	-	5.66	-	23.35	29
Pine Cone Shell	5	25	-	6.81	-	-	30
Spirodela polyrhiza	6.0	-	-	-	36.00	-	31
	4.0	-	-	-	-	137	
Almond shell	7.0	-	22.22	-	-	-	32
Styrene-divinylbenzene allylmethacrylate (SDBAM)	4.0	20	-	-	-	84	33
Cell-*g*-PGMA-PEI	2.0–7.0	28	-	102.24	-	-	34

Table VII. Physical Parameters of Tururi Fiber and of the Fixed-Bed (Column)

Property	Tururi fiber
Column diameter (d_L) (cm)	1.0
Bed height (cm)	9.5
Volume of the empty column (V_L) (cm^3)	7.5
Mass of biosorbent in the column (g)	2.0
Apparent density (ρ_{ap}) (g cm^{-3})	0.64
Packing density (ρ_E) (g cm^{-3})	0.18
Particle volume (V_{ap}) (cm^3)	3.12
Porosity of the bed (ε)	0.73
Hydraulic retention time (min)	3.75
Hydraulic loading (mL min^{-1} cm^{-2})	2.54

The adsorption capacities (q_{max}) followed the order: $Pb^{2+} > Cd^{2+} > Ni^{2+} > Cu^{2+}$. According to the literature, low C_e values best fit to the Langmuir isotherm.[20,26] It is observed from Figure 8 that the adsorption of lead and cadmium metals is favored, especially for lead, while for nickel and copper ions is similar.

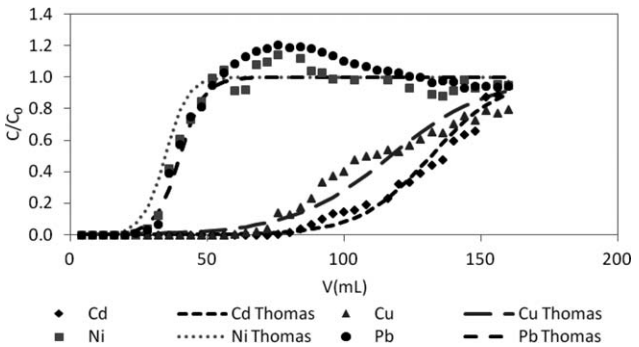

Figure 10. Experimental and theoretical breakthrough curves of metal ions.

The Freundlich model considers that adsorption sites have different affinities for the adsorbate, that is, the adsorption occurs onto a heterogeneous surface and sites with stronger attractive forces are occupied first.[27,28] It is well-known that favorable adsorption processes are associated to "1/n" values between 0.1 and 1. "1/n" was found to be in this range for all metal ions studied.

For a better comparison of the binding affinities, adsorption essays were also performed in the multi-element solutions containing the same amounts of each one of the metals studied (Figure 9). As any solid adsorbent has its own surface area, the presence of solutes results in the competition for available adsorption sites. However, some sites are specific, so that not all ions compete for the same adsorption sites. A study on the competition was performed with multi-element solutions, using the Langmuir extended equation. The adsorption capacity using the extended Langmuir equation was 6.74, 30.45, 27.52, and 85.91 for nickel, copper, cadmium, and lead, respectively. However, it is observed experimentally in Figure 9 that these values are in agreement with experimental data. It is easily noticed that the adsorption capacities of metal ions copper and nickel are much larger than the values found experimentally in monoelementar system, that is, they are being promoted. However, cadmium and lead ions are strongly suppressed.

It can be deduced from inspection of Table VI that the tururi fibers showed good adsorption capacities when compared to

Table VIII. Parameters of the Non-Linear Regression Analysis Using the Thomas Model

		q_0 (mg g^{-1})		
Metal ion	K_t (mL min^{-1} mg^{-1})	Theoretical	Experimental	ERRSQ
Cd^{2+}	0.502	20.0	18.2	0.000
Cu^{2+}	0.400	16.2	16.3	0.000
Ni^{2+}	1.600	5.3	6.4	0.463
Pb^{2+}	1.498	6.0	6.3	2.24

Table IX. Parameters for Breakthrough Curves

Metal ion	V_b (mL)	V_x (mL)	BUR (g L^{-1})	t_x (min)	t_δ (min)	t_f (min)	f	δ (cm)	% SAT
Cd^{2+}	80.0	160.0	25	80.0	40.0	25.5	0.363	0.7	53.3
Cu^{2+}	76.0	160.0	26	80.0	42.0	26.4	0.372	0.8	50.8
Ni^{2+}	32.0	52.0	63	26.0	10.0	7.6	0.243	0.5	58.9
Pb^{2+}	32.0	52.0	63	26.0	10.0	7.9	0.207	0.6	56.1

other adsorbents. This may be related to the experimental conditions and also to the structure of the adsorbents as well as to the affinity of the metal ions for the functional groups present on the adsorbent surface.

Fixed-Bed Experiments

Results for determination of some physical properties of the adsorbent are summarized in Table VII. The hydraulic retention time, being the ratio between the volume and the flow rate, was 3.75 min in this study. The hydraulic loading, being the ratio between the flow rate and the cross-sectional area, was 2.54 mL min^{-1} cm^{-2}, meaning that, each minute, 2.54 mL of solution passed through 1 cm of the cross-sectional area of the fixed bed.

Breakthrough curves for the adsorption of the metal ions studied onto the column are shown in Figure 10. The adsorption capacities calculated with eq. (13) were 18.2, 16.3, 6.4, and 6.3 mg g^{-1} for Cd^{2+}, Cu^{2+}, Ni^{2+}, and Pb^{2+}, respectively. The on-column removal efficiencies column followed the order: $Cd^{2+} > Cu^{2+} > Ni^{2+} > Pb^{2+}$.

In the case of multi-element systems at the initial stage, there is a large amount of active sites and the metal ions which can be strongly and weakly adsorbed occur onto active sites that are freely accessible. With the advancement of time, weakly adsorbed ions move with the fluid and occupy the active sites first in the front part of the fixed bed. The strongly adsorbed metal ions tend to adsorb onto the active sites occupied by weakly adsorbed metal ions thereby displacing them. As a result, the concentrations of the weakly adsorbed metal ions are higher in the fluid phase of the fixed-bed adsorbent.[35] Consequently, the weakly adsorbed metal ions elute from the column resulting in a final concentration higher than the initial one. This can be observed from the curves of Pb^{2+} and Ni^{2+}, which, upon reaching saturation ($C/C_{in} = 1$), start to elute giving room for Cu^{2+} and Cd^{2+} that are more strongly adsorbed and whose curves show the profile of a common rupture curve.

The Thomas model was applied to the experimental data. Nonlinear regression analysis was performed using eq. (14). The ERRSQ was examined for each experimental dataset and the parameters of K_{TH} and q_{TH} were determined for the lowest error values in each case by adjusting and optimizing the functions themselves using the solver add-in for Microsoft Excel®. The values of K_{TH} and q_{TH} obtained for the lowest error values are displayed in Table VIII.

The Thomas model represented the data well, especially for Cd^{2+} and Cu^{2+}. In general, the theoretical and experimental maximum adsorption capacities were close. With the values of K_{TH} and q_{TH} for each metal ion, the total mass of adsorbent required to treat wastewater using a fixed bed (column) can be obtained under the same conditions, requiring only knowledge of the feed concentration for each metal ion, the daily flow rate, and the volume of solution to be treated.

The values obtained from the breakthrough curves were used to calculate parameters t_x, t_δ, t_f, f, δ, and the percentages of saturation of the column, as given in Table IX. The total times to establish the primary adsorption zone (t_x) were 80 min for Cd^{2+} and Cu^{2+}, and 26 min for Ni^{2+} and Pb^{2+}. The times required to move the adsorption zone down the column (t_δ)

Table X. Comparison of Adsorption Capacities of Metal Ions Using Various Adsorbents in Fixed-Bed (Column)

	q (mg g^{-1})						
Adsorbent	Cu^{2+}	Pb^{2+}	Ni^{2+}	Cd^{2+}	pH	Fixed-bed height (cm)	Reference
Tururi fiber	16.30	6.30	6.40	18.20	5.5	9.5	This work
Green coconut shell	20.26	11.96	3.12	17.90	5.0	10	8
Modified activated carbon	38.00	-	-	-	-	20	36
Immobilized fungal biomass	-	-	1.08	-	5.0–7.0	24.5	37
Chitosan-8-hydroxyquinoline	7.96	-	9.97	-	5.0	3	38
Crab shell particles	52.07	-	-	-	6.0	25	39
Manganese oxide coated zeolite	0.12	-	-	1.12	5.0	15	40
Tea waste	48.00	-	-	65.00	5–6	10	41
Penicillium membrane	10.69	-	-	-	-	6.29	42
rice straw powder	-	-	75	-	-	2	43

are situated between 10 and 42 min. The times required for initial formation of the primary adsorption zone (t_f) are between 26.4 and 7.6 min. The adsorbent usage rate, that is, the adsorbent weight in the column divided by the amount of liquid passed into the column at the time when breakthrough occurs, was found to be 63 g (minimum) to treat 1 L of an effluent containing the four metal ions studied in the specified concentrations. The adsorption capacities obtained for tururi fibers in fixed-bed systems were compared with other adsorbents that have been used for the treatment of toxic metal ions (Table X). The use of tururi fibers can be considered as a cheap and efficient renewable biosorbent for use in the treatment of industrial aqueous effluents.

CONCLUSIONS

The most effective adsorption and removal of metal ions Cd^{2+}, Cu^{2+}, Ni^{2+}, and Pb^{2+} from aqueous solutions were found for tururi fibers modified with 7% (w/v) sodium hydroxide. Experimental design results showed that the factors studied influenced each metal adsorption differently. The maximum total adsorption, according to the fitted model, is obtained maintaining factors pH, agitation rate, and initial metal concentration at higher level, 5.5; 200 rpm and 300 mg g^{-1}, respectively. The factor adsorbent mass at lower level was 50 mg. The adsorption kinetics indicated that the multi-element adsorption equilibrium was reached within 15 min for all metal ions studied and that the experimental data best fitted to the pseudo-second order kinetic model. The analysis of the isotherms by the non-linear model showed that the experimental data for Cd^{2+}, Cu^{2+}, Ni^{2+}, and Pb^{2+} were best described by the Langmuir model as high R^2 and low ERRSQ values were obtained. The maximum adsorption capacities followed the order: Cu^{2+} (36.36) > Cd^{2+} (156.87) > Pb^{2+} (346.28) > Ni^{2+} (50.12). Breakthrough curves revealed that saturation of the bed was reached in 160.0 mL with Cd^{2+} and Cu^{2+}, and 52.0 mL with Ni^{2+} and Pb^{2+}. The Thomas model was applied to the experimental data of breakthrough curves and represented the data well. The tururi fiber is favorable adsorbent for industrial applications of heavy metals wastewater treatment.

ACKNOWLEDGMENTS

The authors are grateful to FUNCAP (Fundação Cearense de Apoio ao Desenvolvimento Científico e Tecnológico), CAPES (Coordenação de Aperfeiçoamento de Pessoal de Nível Superior), and CNPq (Conselho Nacional de Desenvolvimento Científico e Tecnológico) for grants and fellowships.

AUTHOR CONTRIBUTIONS

Ms. Diego Quadros Melo conducted the experiments of batch and fixed bed and wrote the manuscript; Ms. Raimundo N. P. Teixeira performed IV experiments; Ms. Giselle Santiago Cabral Raulino and Carla Bastos Vidal performed factorial design experiments and wrote the manuscript; Mr. André Leandro da Silva performed of Influence of alkaline treatments experiments; Ms. Thiago C. Medeiros conducted the data processing of factorial design in Minitab software and interpretation of data; Dr. Selma Elaine Mazzeto interpretation of data; Pierre Basílio Almeida Fechine performed MEV and data discussion. Dr. Denis De Keukeleire conducted a review of language and revising it critically; Dr. Ronaldo Ferreira do Nascimento supervised the research and revising it critically.

REFERENCES

1. Baird, C. Química Ambiental; Editora Bookman: Porto Alegre, **2002**.
2. Neto, V. O. S.; Carvalho, T. V.; Honorato, S. B.; Gomes, C. L.; Freitas, F. C.; Silva, M. A. A.; Freire, P. T. C.; Nascimento, R. F. *Bioresources* **2012**, *7*, 1504.
3. Hubbe, M. A.; Hasan, S. H.; Ducoste, J. J. *Met. Bioresour.* **2011**, *6*, 2161.
4. Sousa, F. W.; Silva, M. J. B.; Oliveira, I. R. N.; Oliveira, A. G.; Cavalcante, R. M.; Fechine, P. B. A.; Sousa Neto, V. O.; De Keukeleire, D.; Nascimento, R. F. *J. Environ. Manage.* **2009**, *89*, 1.
5. Sanchez, R. A.; Espósito, B. P. *Bioresources* **2011**, *6*, 2448.
6. Moreira, S. A.; Sousa, F. W.; Oliveira, A. G.; Brito, E. S.; Nascimento, R. F. *Quim. Nova* **2009**, *32*, 1717.
7. Sousa, F. W.; Moreira, S. A.; Oliveira, A. G.; Cavalcante, R. M.; Nascimento, R. F.; Rosa, M. F. *Quim. Nova* **2007**, *30*, 1153.
8. Sousa, F. W.; Oliveira, A. G.; Ribeiro, J. P.; Rosa, F. M.; De Keukeleire, D.; Nascimento, R. F. *J. Environ. Manage.* **2010**, *91*, 1634.
9. Sousa, F. W.; Oliveira, A. G.; Ribeiro, J. P.; De Keukeleire, D.; Sousa, A. F.; Nascimento, R. F. *Desalination Water Treat.* **2011**, *36*, 289.
10. Kasgoz, H.; Ozbas, Z.; Esen, E.; Sahin, C.P.; Gurdag, G. *J. Appl. Polym. Sci.* **2013**, *130*, 4440.
11. Fernandez, N. B.; Mullassery, M. D.; Anirudhan, T S. *J. Appl. Polym. Sci.* **2012**, *125*, 262.
12. Moura, C. P.; Vidal, C. B.; Barros, A. L.; Costa, L. S.; Vasconcellos, L. C. G.; Dias, F. S.; Nascimento, R. F. *J. Colloid Interface Sci.* **2011**, *363*, 626.
13. Cooney, D.O. Adsorption Design for Wastewater Treatment. CRC Press: Boca Raton, FL, **1999**.
14. Gupta, V. K.; Srivastava, S. K.; Mohan, D.; Sharma, S. *Waste Manag.* **1997**, *17*, 517.
15. Kundu, S.; Gupta, A. K. *J. Colloid Interface Sci.* **2005**, *290*, 52.
16. Melo, D. Q.; Gomes, E. C. C.; Raulino, G. S. C.; Longhinotti, E.; Nascimento, R. F. *J. Chem. Eng. Data* **2013**, *58*, 798.
17. Jin, H.; Zha, C.; Gu, L. *Carbohydr. Res.* **2007**, *342*, 851.
18. Kroon-Batenburg, L. M. J.; Kroon, J. *Glycoconj. J.* **1997**, *14*, 677.
19. Box, G. E.; Hunter, W. G.; Hunter, J. S. Statistics for Experiments; Wiley: New York, **1978**.
20. Vidal, C. B.; Barros, A. L.; Moura, C. P.; De Lima, A. C. A.; Dias, F. S.; Vasconcellos, L. C. G.; Fechine, P. B. A.; Nascimento; R. F. *J. Colloid Interface Sci.* **2011**, *357*, 466.
21. Loukidou, M. X.; Karapantsios, T. D.; Zouboulis, A. I.; Matis, K. A. *J. Chem. Technol. Biotechnol.* **2004**, *7*, 711.

22. Teixeira, R. N. P.; Sousa Neto, V. O.; Oliveira, J. T.; Melo, D. Q.; Araujo-Silva, M. A.; Nascimento, R. F. *Bioresources* **2013**, *8*, 3356.

23. Areco, M. M.; Hanelab, S.; Duranb, J.; Dos Santos, A. M. *J. Hazard. Mater.* **2012**, *213–214*, 123.

24. Ajaelu, C. J.; Ibironke, O. L.; Adedeji, V.; Olafisoye, O. *Am.-Eurasian J. Sci. Res.* **2011**, *6*, 123.

25. Sarıa, A.; Tuzen, M. *J. Hazard. Mater.* **2009**, *164*, 1004.

26. Vidal, C. B.; Raulino, G. S. C.; Barros, A. L.; Lima, A. C. A.; Ribeiro, J. P.; Pires, M. J. R.; Nascimento, R. F. *J. Environ. Manage.* **2012**, *112*, 178.

27. Febrianto, J.; Kosasih, A. N.; Sunarso, J.; Ju; Y. H.; Indraswati, N.; Ismadji, S. *J. Hazard. Mater.* **2009**, *162*, 616.

28. Han, R.; Zhang, J.; Han, P.; Wang, Y.; Zhao, Z.; Thang, M. *Chem. Eng. J.* **2009**, *145*, 496.

29. Soetaredjo, F. E; Kurniawan, A.; Ki, O. L.; Ismadji, S. *Chem. Eng. J.* **2013**, *219*, 137.

30. Blázquez, G.; Martín-Lara, M. A.; Dionisio-Ruiz, E.; Tenorio, G.; Calero M. *J. Ind. Eng. Chem.* **2012**, *18*, 1741.

31. Meitei, M. D.; Prasad, M. N. V. *J. Environ. Chem. Eng.* **2013**, *1*, 200.

32. Kilic, M.; Kirbiyik, Ç.; Cepeliogullar, Ö.; Pütün, A. E. *Appl. Surf. Sci.* **2013**, *283*, 856.

33. Ahmetli, G.; Yel, E.; Deveci, H.; Bravo, Y.; Bravo, Z. *J. Appl. Polym. Sci.* **2012**, *125*, 716.

34. Tang, Y.; Ma, Q.; Luo, Y.; Zhai, L.; Che, Y.; Meng, F. *J. Appl. Polym. Sci.* **2013**, *129*, 1799.

35. Sulaymon, A. H.; Ahmed, K. W. *Environ. Sci. Technol.* **2008**, *42*, 392.

36. Monser, L.; Adhoum, N. *Sep. Purif. Technol.* **2002**, *26*, 137.

37. Kapoor, A.; Viraraghavan, T. *Water Res.* **1998**, *32*, 1968.

38. Barros, F. C. F.; Sousa, F. W.; Cavalcante, R. M.; Carvalho, T. V.; Dias, F. S.; Queiroz, D. C.; Vasconcellos, L. C. G.; Nascimento, R. F. *Clean—Soil Air Water* **2008**, *36*, 292.

39. Vijayaraghavan, K.; Thilakavathi, M.; Palanivelu, K.; Velan, M. *Environ. Technol.* **2005**, *26*, 267.

40. Han, R.; Zou, W.; Li, H.; Li, Y.; Shi, J. *J. Hazard. Mater. B* **2006**, *137*, 934.

41. Amarasinghe, B. M. W. P. K.; Williams, R. A. *Chem. Eng. J.* **2007**, *132*, 299.

42. Xiao, G.; Zhang, X.; Su, H.; Tan, T. *Bioresour. Technol.* **2013**, *143*, 490.

43. Sharma, R.; Singh, B. *Bioresour. Technol.* **2013**, *146*, 519.